Solving Variational Problems and Partial Differential Equations Mapping into General Target Manifolds*

Facundo Mémoli†
ECE Dept.
University of Minnesota,
Minneapolis, MN 55455
e-mail: memoli@ece.umn.edu

Guillermo Sapiro
ECE Dept.
University of Minnesota,
Minneapolis, MN 55455
e-mail: guille@ece.umn.edu

Stanley Osher
Mathematics Dept.
UCLA,
Los Angeles, CA 90095
email: sjo@math.ucla.edu

Abstract

A framework for solving variational problems and partial differential equations that define maps onto a given generic manifold is introduced in this paper. We discuss the framework for arbitrary target manifolds, while the domain manifold problem was addressed in [3]. The key idea is to implicitly represent the target manifold as the zero level-set of a higher dimensional function, and then implement the equations in the Cartesian coordinate system where this embedding function is defined. In the case of variational problems, we restrict the search of the minimizing map to the class of maps whose target is the level-set of interest. In the case of partial differential equations, we re-write all the equation's geometric characteristics with respect to the implicitation function. We then obtain a set of equations that while defined on the whole Euclidean space, are intrinsic to the implicitly defined target manifold and map into it. This permits the use of classical numerical techniques in Cartesian grids, regardless of the geometry of the target manifold. The extension to open surfaces and submanifolds is addressed in this paper as well. In the latter case, the submanifold is defined as the intersection of two higher dimensional surfaces, and all the computations are restricted to this intersection. Examples of the applications of the framework here described include harmonic maps in liquid crystals, where the target manifold is an hypersphere; probability maps, where the target manifold is an hyperplane; chroma enhancement; texture mapping; and general geometric mapping between high dimensional surfaces.

1 Introduction

In a number of applications in mathematical physics, image processing, computer graphics, and medical imaging, we have to solve variational problems and partial differential equations defined on a general manifold $\mathcal{M}$ (*domain manifold*), which map the data onto another general manifold $\mathcal{N}$ (*target manifold*). That is, we deal with maps from $\mathcal{M}$ to $\mathcal{N}$. When these manifolds are for example three dimensional surfaces, the implementation of the corresponding gradient descent flow or the given PDE's is considerably elaborate. In [3] we have shown how to address this problem for general domain manifolds, while restricting the target manifolds $\mathcal{N}$ to the trivial cases of the Euclidean space or hyper-spheres (this framework has been followed for example in [2]). The key idea was to implicitly represent the domain surface as the (zero) level-set of a higher dimensional function ϕ, and then solve the PDE in the Cartesian coordinate system which contains the domain of this new embedding function. The technique was justified and demonstrated in [3]. It is the goal of this paper (see [18] for details and proofs), to show how to work with general target manifolds, and not just hyperplanes or hyper-spheres as previously reported in the literature. Inspired by [3], we also embed the target manifold $\mathcal{N}$ as the (zero) level-set of a higher dimensional function ψ. That is, when solving the gradient descent flow (or in general, the PDE), we guarantee that the map receives its values on the zero level-set of ψ. The map is defined on the whole space, although it never receives values outside of this level-set. Examples of applications of this framework include harmonic maps in liquid crystals ($\mathcal{N}$ is an hypersphere) and 3D surface warping [26]. In this last case, the basic idea is to find a smooth map between two given surfaces. Due to the lack of the new frameworks introduced here and in [3], this problem is generally addressed in the literature after an intermediate mapping of the surfaces onto the plane is performed (see also [14, 28]). With these novel frameworks, direct three dimensional maps can be computed without any intermediate mapping, thereby eliminating their corresponding geometric distortions [19]. For this application, as in [26], boundary conditions are needed, and how to add them to the frameworks introduced here and in [3] is addressed in [19].

To introduce the ideas, in this paper we concentrate on flat domain manifolds.[1] When combining this framework with

*This work was partially supported by ONR and NSF. The resarch of F.M. is also supported by CSIC-Uruguay.

†F.M. is also with the Instituto de Ingeniería Eléctrica, Facultad de Ingeniería, Universidad de la República, Uruguay.

[1]For completeness, we will present the general equations for both

the results on [3], we can of course work with general domains and then completely avoid other popular surface representations, like triangulated surfaces. We are then able to work with intrinsic equations, in Euclidean space and with classical numerics on Cartesian grids, regardless of the geometry of the involved domain and target manifolds. In addition to presenting the general theory, we also address the problem of target submanifolds and open surfaces. A number of theoretical results complement the algorithmic framework here described.

For illustration purposes only, the proposed framework is presented for classical equations from the theory of harmonic maps. The technique can easily be extended to general equations, as it will be clear from the developments below.

1.1 Why implicit representations?

Let us conclude this introduction describing the main advantages of working with implicit representation when dealing with PDE's and variational problems.

The implicit representation of surfaces here introduced for solving variational problems and PDE's is inspired in part by the level-set work of Osher and Sethian [20]. This work, and those that followed it, showed the importance of representing deforming surfaces as level-sets of functions with higher dimensional domains, obtaining more robust and accurate numerical algorithms (and topological freedom). Note that, in contrast with the level-set approach of Osher and Sethian, our target manifold is fixed, what is "deforming" is the dataset being mapped onto it.

Solving PDE's and variational problems with polynomial meshes involves the non-trivial discretization of the equations in general polygonal grids, as well as the difficult numerical computation of other quantities like projections onto the discretized surface (when computing gradients and Laplacians for example). Although the use of triangulated surfaces is quite popular, there is still no consensus on how to compute simple differential characteristics such as tangents, normals, principal directions, and curvatures. On the other hand, it is widely accepted that computing these objects for iso-surfaces (implicit representations) is straightforward and much more accurate and robust. This problem becomes even more significant when we not only have to compute these first and second order differential characteristics of the surface, but also have to use them to solve variational problems and PDE's for data defined on the surface. Note also that working with polygonal representations is dimensionality dependent, and solving these equations for high dimensional (> 2) surfaces becomes even more challenging.

Our framework of implicit representations enables us to perform all the computations on the Cartesian grid corresponding to the embedding function. These computations are, nevertheless, intrinsic to the surface. Advantages of using Cartesian grid instead of a triangulated mesh include the availability of well studied numerical techniques with accurate error measures and the topological flexibility of the surface, all leading to simple, accurate, robust and elegant implementations. The approach is dimensionality independent as well. As mentioned above, problems such as 3D shape warping via PDE's could not be addressed (without intermediate projections) without the framework here proposed.

Numerical schemes that solve gradient descent flows and PDE's onto generic target manifolds $\mathcal{N}$ (and spheres or surfaces in particular) will, in general, move the points outside of $\mathcal{N}$ due to numerical errors. The points will then need to be projected back,[2] see for example [1, 6] for the case of $\mathcal{N}$ being a sphere (where the projection is trivial, just a normalization). For general target manifolds, this projection means that for every point $p \in I\!R^d$ ($\mathcal{N} \subset I\!R^d$) we need to know the closest point to p in $\mathcal{N}$. This means knowing the distance from every point $p \in I\!R^d$ to $\mathcal{N}$ (or at least all points in a band of $\mathcal{N}$). This is nothing else than an implicit representation of the target $\mathcal{N}$, being the particular embedding in this case a distance function. This presents an additional justification for the framework here introduced, that is, if the embedding function for the surface has to be computed anyway, why not use it from the beginning if it helps in the numerical computations?

In a number of applications, surfaces are already given in implicit form, e.g., [4], therefore, the framework introduced in this paper is not only simple and robust, but it is also natural in those applications. Moreover, in the state-of-the-art and most commonly used packages to obtain 3D models from range data, the algorithms output an implicit (distance) function (see for example graphics.stanford.edu/projects/mich/). On the other hand, not all surfaces (manifolds) are originally represented in implicit form. When the target manifold $\mathcal{N}$ is simple, like hyperspheres in the case of liquid crystals, the implicitation process is trivial. For generic surfaces, we need to apply an algorithm that transforms the given explicit representation into an implicit one. Although this is still a very active area of research, many very good algorithms have been developed, e.g., [8, 11, 16, 27]. Note that this translation needs to be done only once for any surface. Note also that for rendering, the volumetric data can be used directly, without the need for an intermediate mesh representation.

2 The Computational Framework

From now on we assume that the target $d-1$ dimensional manifold $\mathcal{N}$ is given as the zero level set of a higher dimensional embedding function $\psi : I\!R^d \rightarrow I\!R$, which we consider to be a signed distance function (this mainly simplifies the notation). For the case where $\mathcal{N}$ is a surface in three

generic domain and target manifolds at the end of the paper. These equations are easily derived from [3] and the work presented in this paper.

[2] For particular flat target manifolds as the whole space $I\!R^d$ or as those in [21], the projection is not needed. Other authors, e.g., [5, 15], have avoided the projection step for particular cases, while in [30] the authors modify the formulation, in some restricted cases (namely 2D), to include the projection step.

dimensional space for example, then $\psi : \mathbb{R}^3 \rightarrow \mathbb{R}$. We also assume that the domain manifold $\mathcal{M}$ is flat and open (as mentioned in the introduction, general domain manifolds were addressed in [3]). We illustrate the basic ideas with a functional from the theory of harmonic maps. This is just a particular example (and a very important one), and from this example it will be clear how the same arguments can be applied to any given variational problem and PDE. In particular, it can be applied to common Navier-Stokes flows used in brain warping [19].

2.1 The Variational Formulation and its Euler-Lagrange

We search for necessary conditions for the functional $E[\vec{u}]$, defined by

$$E[\vec{u}] \stackrel{\triangle}{=} \int_{\mathcal{M}} e[\vec{u}]\, d_{\mathcal{M}} v \tag{1}$$

where

$$e[\vec{u}] \stackrel{\triangle}{=} \frac{1}{2} \|\mathbf{J}_{\vec{u}}\|^2_{\mathcal{F}} \tag{2}$$

to achieve a minimum. Here, $\|\cdot\|^2_{\mathcal{F}} = \sum_{ij} (\cdot)^2_{ij}$ is the norm of Frobenius and $\mathbf{J}_{\vec{u}}$ is the Jacobian of the map $\vec{u} : \mathcal{M} \rightarrow \{\psi = 0\}$. Note that here we are already restricting the map to be onto the zero level-set of ψ, that is, onto the surface of interest $\mathcal{N}$ (the target manifold). This is what permits us to work with the embedding function and the whole space, while guaranteeing that the map will always be onto the target manifold, as desired.[3] Once again, this energy will be used throughout this paper to exemplify our framework. It will be clear after developing this example that the same arguments work for other variational formulations, as well as for generic PDE's defined onto generic surfaces.

Proposition 1 ([18]) *The Euler-Lagrange of Equation (1), with (2), is given by*

$$\Delta \vec{u} + \left(\sum_k \mathbf{H}_\psi \left[\frac{\partial \vec{u}}{\partial x_k}, \frac{\partial \vec{u}}{\partial x_k} \right] \right) \nabla \psi(\vec{u}) = 0, \tag{3}$$

where $\mathbf{H}_\psi$ stands for the Hessian of the embedding function ψ (and we used the notation $A\,[\vec{x}, \vec{y}] = \vec{y}^T A\, \vec{x}$). The solution to this equation is a map onto the zero level-set of ψ.

This equation then gives the corresponding Euler-Lagrange for the given variational problem (and from it we get the gradient-descent flow, with Neumann boundary conditions). Note, once again from our computations, that despite all the terms "live" in the Euclidean space where the target manifold is embedded, $\vec{u}$ will always map onto the level-set of interest, $\{\psi = 0\}$, and therefore, onto the surface of interest. This is guaranteed by this equation, no additional computations are needed. This is the beauty of the approach, while working freely on the Euclidean space (and therefore with Cartesian numerics), we can guarantee that the equations are intrinsic to the given surfaces of interest. We will further verify this in §2.2 to help the reader grasp the intuition behind this framework.

[3] We use $\vec{\cdot}$ to note that for the most general case, the function is vectorial.

2.2 Simple Verifications

We now show that the Euler-Lagrange above, and its corresponding gradient descent flow, are the extension for implicit targets of common equations derived in the literature for explicitly represented manifolds. We also explicitly show that the flow equation guarantees, as expected from the derivations above and in particular from the proof of Proposition 1, that if the initial datum is on the target manifold, it will remain on it. We also express the second fundamental form of a manifold that is implicitly represented. All these results will help to further illustrate the approach and verify its correctness.

Geodesics on Implicit Manifolds

It is well known, see [9, 10, 23], that arc-length parameterized geodesics on the manifold $\mathcal{N}$ satisfy the harmonic maps PDE, and therefore Equation (3). If we assume isotropic and homogeneous metric over $\mathcal{N}$, from Equation (3) we obtain that (arc-length parameterized) geodesics must satisfy

$$\ddot{\gamma} + \mathbf{H}_\psi\, [\dot{\gamma}, \dot{\gamma}]\ \nabla \psi(\gamma) = 0. \tag{4}$$

This important equation shows how to obtain geodesic curves on manifolds represented in implicit form.

Liquid Crystals

One of the most popular examples of harmonic maps is given when the target manifold $\mathcal{N}$ is an hypersphere. That is, the map is onto S^{d-1}. In this case, the embedding (signed distance) function is simply $\psi(\vec{y}) = \|\vec{y}\| - 1$, $\vec{y} \in \mathbb{R}^d$. From this, $\nabla \psi(\vec{y}) = \frac{\vec{y}}{\|\vec{y}\|}$ and $(\mathbf{H}_\psi(\vec{y}))_{ij} = \frac{\delta_{ij}}{\|\vec{y}\|} - \frac{y_i y_j}{\|\vec{y}\|^3}$. We also have that $\mathbf{H}_\psi(\vec{u}(x)) \left[\frac{\partial \vec{u}}{\partial x_k}, \frac{\partial \vec{u}}{\partial x_k} \right] = \delta_{ij} \frac{\partial u^i}{\partial x_k} \frac{\partial u^j}{\partial x_k} - \frac{\partial u^i}{\partial x_k} \frac{\partial u^j}{\partial x_k} u_i u_j$, since $\|\vec{u}\| = 1$. In addition, $u^i \frac{\partial u^i}{\partial x_k} = 0$, fact simply obtained taking derivatives with respect to x_k. We then obtain that $\frac{\partial u^i}{\partial x_k} \frac{\partial u^j}{\partial x_k} u_i u_j = \left(\frac{\partial u^i}{\partial x_k} u_i \right)^2 = 0$, and $\sum_{k=1}^d \mathbf{H}_\psi(\vec{u}(x)) \left[\frac{\partial \vec{u}}{\partial x_k}, \frac{\partial \vec{u}}{\partial x_k} \right] = \sum_{ik} \left(\frac{\partial u^i}{\partial x_k} \right)^2$ which equals $\|\mathbf{J}_{\vec{u}}(x)\|^2_{\mathcal{F}}$. Therefore, following the general Euler-Lagrange equation, the corresponding diffusion equation for this particular case is

$$\frac{\partial \vec{u}}{\partial t} = \Delta \vec{u} + \|\mathbf{J}_{\vec{u}}\|^2_{\mathcal{F}}\ \vec{u}$$

which is exactly the well known gradient descent flow for this case. We have then verified the correctness of the derivation in Proposition 1 for the case of unit spheres as target manifolds.

Mapping Restriction onto the Zero Level-Set

We now explicitly show that if the initial datum belongs to the target surface given by the zero level-set of ψ, then the solution to the gradient descent flow corresponding to (3) also belongs to this level-set. This further shows the correctness of our approach.

Proposition 2 ([18]) *A regular solution to the gradient descent flow corresponding to Equation (3) holds* $\psi(\vec{u}(x,t)) = 0,\ \forall\, x \in \mathcal{M},\ \forall\, t \geq 0$ *of regularity.*

Second Fundamental Form for Implicit Surfaces

If we compare the gradient descent flow (and Euler-Lagrange equation) we have obtained with the classical one from harmonic maps, we see that the main difference is that Christoffel symbols for the target manifold term appearing in the classical formulation have been replaced by a new term that includes the Hessian of the embedding function. We obtained this by first implicitizing the target manifold and then restricting the search for the minimizing map to the class of maps onto the zero level-set of the embedding function. This approach can be followed to apply this framework to any related variational problem. The same equation can be obtained by simply substituting the second fundamental form of the explicit target manifold by the corresponding expression for an implicit target manifold [18] (see also §4). This illustrates how to apply our framework to more general PDE's, not necessarily gradient descent flow. The basic idea is just to replace all the PDE components concerning the target manifold by their counterparts for implicit representations.

2.3 Maps into Open Surfaces

So far, we have only addressed the case when the target surface is closed (zero level-set). We now briefly deal with open surfaces. We show, following classical results, that when the map $\vec{u}$ is evolving according to the flow from (3), the set $\mathcal{C}(t) \stackrel{\triangle}{=} \{\vec{u}(x,t),\ x \in \mathcal{M}\}$ remains inside the initial *convex-hull* of $\mathcal{C}_0 \stackrel{\triangle}{=} \{\vec{u}_0(x),\ x \in \mathcal{M}\}, \forall\, t \geq 0$. This property is basically a consequence of the maximum principle.

Let us first motivate the general result presented below for the planar case. Assume that the target manifold $\mathcal{N}$ is flat, for example R^k (we still assume that the domain manifold $\mathcal{M}$ is flat). Let $\vec{u}(x,t)$ solve $\frac{\partial \vec{u}}{\partial t} = \Delta \vec{u}$ for $x \in \mathcal{M}$ and $t \geq 0$, and $\frac{\partial \vec{u}}{\partial \mathbf{n}}\big|_{\partial \mathcal{M}} = 0$. Let Ξ be a convex set of R^k with smooth boundary (this guarantees that the distance function is also smooth almost everywhere, see [23] for a formal statement), and ξ the signed distance function to this set (positive outside and negative inside). Define $g(x,t) \stackrel{\triangle}{=} \xi(\vec{u}(x,t))$. Then it follows that $\frac{\partial g}{\partial t} - \Delta g = -\sum_{i=1}^{k} \mathbf{H}_\xi(\frac{\partial \vec{u}}{\partial x_k}, \frac{\partial \vec{u}}{\partial x_k})$.[4]

[4]Note that we are omitting details regarding the correct handling of the distance function, since it is not everywhere differentiable. However, by a regularization argument, the same conclusion holds.

Since Ξ is convex, so it is ξ. Then, the *Hessian* of ξ is *positive semi-definite*, meaning that $\frac{\partial g}{\partial t} - \Delta g \leq 0$. Following the scalar maximum principle, $\max_{\{x \in \mathcal{M},\, t \geq 0\}} g(x,t) = \max_{\{x \in \mathcal{M}\}} g(x,0)$. If $\{\vec{u}_0(x),\ x \in \mathcal{M}\} \subseteq \Xi$, which is equivalent to $0 \geq \xi(\vec{u}_0(x)) = g(x,0)$, we obtain that $g(x,t) \leq 0$, and $\vec{u}(x,t) \in \Xi$, for all $x \in \mathcal{M}$ y $t \geq 0$.

The general result now presented is from [13]. We quote it here for completeness.[5]

Theorem 1 *Let* $\vec{u}(x,t)$ *be the solution of the gradient descent flow corresponding to (3) at time* t*. Let us assume that for* $t \leq T$ *this solution remains smooth. Let* $I_0 = \vec{u}_0(\Omega)$*, and* $\mathcal{I}_0$ *be the* convex hull *of* I_0*. Then for* $(x,t) \in \Omega \times [0,T]$*,* $\vec{u}(x,t) \in \mathcal{I}_0$*.*

3 Maps onto Implicit Submanifolds

Here we present a modification to the diffusion flow introduced above, which is well suited to diffuse data that belongs to a certain *submanifold* $\mathcal{C}$ of $\mathcal{N} = \{\psi = 0\}$. We specify this submanifold by $\{\psi = 0\} \cap \{\Phi = 0\}$, where we select $\Phi : I\!R^N \to R$ to be the signed *intrinsic* (to $\mathcal{N}$) distance function to $\{\Phi = 0\}$, satisfying

$$1 = \|\nabla_\psi \Phi\| = \sqrt{\|\nabla \Phi\|^2 - |\nabla \psi \cdot \nabla \Phi|^2} \qquad (5)$$

In addition we specify the condition

$$\Phi(p) = 0 \text{ for } p \in \mathcal{K}_\Phi$$

where

$$\mathcal{K}_\Phi = \{x \in I\!R^N \mid x = p + \alpha \nabla \psi(p), \text{with } p \in \mathcal{C},\ \alpha \in I\!R\}$$

is the *cone* intersecting $\{\psi = 0\}$ at $\mathcal{C}$ and director rays normal also to $\{\psi = 0\}$.

The reason for specifying the submanifold this way is that we cannot proceed as before, simply specifying the submanifold as the zero level set of it's Euclidean distance function. This is because such function would be singular precisely on the submanifold.

As we show in [18], the Hessian of Φ, *intrinsic* to $\mathcal{N}$ evaluated at the point p, and restricted to act on vectors that belong to $T_p\mathcal{N}$ (tangent space), can be written in the form

$$\mathbf{H}_\Phi^{\mathcal{N}}(p) = \mathbf{H}_\Phi(p) - \Lambda(p)\ \mathbf{H}_\psi(p) \qquad (6)$$

where $\Lambda(p) = \nabla \Phi(p) \cdot \nabla \psi(p)$. This expression will be used below.

We now derive the Euler-Lagrange corresponding to this additional mapping restriction.

[5]The proof of this result has a lot of interest in itself since it can be carried out within the implicit framework introduced in this paper.

Proposition 3 ([18]) *The Euler-Lagrange of the functional (1), when the solution is restricted to the implicitly represented submanifold $\mathcal{C}$ defined above, is given by*

$$\Delta\vec{u} \;+\; \left(\sum_k \mathbf{H}_\psi\left[\frac{\partial\vec{u}}{\partial x_k},\frac{\partial\vec{u}}{\partial x_k}\right]\right)\nabla\psi(\vec{u}) \;+\; \left(\sum_k \mathbf{H}^{\mathcal{N}}_\Phi\left[\frac{\partial\vec{u}}{\partial x_k},\frac{\partial\vec{u}}{\partial x_k}\right]\right)\nabla_\psi\Phi(\vec{u}) = 0. \tag{7}$$

As for the case of closed manifolds, we now verify that in fact the gradient descent corresponding to this Euler-Lagrange equation keeps $\vec{u}$ in $\{\psi=0\}\cap\{\Phi=0\}$.

Proposition 4 ([18]) *If $\vec{u}$ is a solution to the gradient descent flow corresponding to Equation (7), then $\vec{u}$ maps into the submanifold $\{\psi=0\}\cap\{\Phi=0\}$.*

4 Implicit Domain Manifolds and p-Harmonic Maps

For completeness, we present now the formulas corresponding to the case where both the domain and target manifolds are represented in implicit form (with the implicitizing functions being the corresponding signed distance ones). Deriving these formulas is straightforward using the framework here presented when combined with the work in [3]. We also show the corresponding flows for p-harmonic maps.

4.1 p-Harmonic Maps

We still assume $\mathcal{M}$ to be planar. The energy density (2) (but not the dependence of the energy on its density) is redefined as follows. For every $p\in[1,+\infty)$ let

$$e_p[\vec{u}] \triangleq \frac{1}{p}\|\mathbf{J}_{\vec{u}}\|^p_{\mathcal{F}}$$

A simple application of variational calculus leads to conclude that[6]

$$\vec{u}_t = p^{1-\frac{2}{p}}\;\mathbf{\Pi}_{\nabla\psi(\vec{u})}\left(\nabla\cdot\left((e_p[\vec{u}])^{1-\frac{2}{p}}\;\mathbf{J}^T_{\vec{u}}\right)\right) \tag{8}$$

Note that if $p<2$ difficulties are expected to arise, see [24] and the references therein.

4.2 Generic (Implicit) Domain Manifolds

Let $\mathcal{M}=\{x\in\mathbb{R}^m:\phi(x)=0\}$, where $\phi(\cdot)$ is the signed distance function to $\mathcal{M}$, then the diffusion is given by:

$$\vec{u}_t = \nabla\cdot\left(\mathbf{\Pi}_{\nabla\phi}\mathbf{J}^T_{\vec{u}}\right) \;+\; \left(\sum_{k,r}\mathbf{H}_\psi[\vec{u}_{x_r},\vec{u}_{x_k}]\left(\mathbf{\Pi}_{\nabla\phi}\right)_{kr}\right)\nabla\psi \tag{9}$$

[6]The divergence operator convention (for a matrix A) we have used is $\nabla\cdot A=\left(\nabla\cdot\vec{A}_{v1}|\ldots|\nabla\cdot\vec{A}_{vr}\right)$, where $\vec{A}_{vi}$ stands for the i-th column of A. That is, we apply a columnwise divergence.

The whole deduction rests upon the redefinition of the energy (1) and its density (2). Now we should define the energy density to be $e_\phi[\vec{u}]\triangleq\frac{1}{2}\|\mathbf{J}^\phi_{\vec{u}}\|^2_{\mathcal{F}}$, where the *intrinsic Jacobian* of $\vec{u}$ can be written as $\mathbf{J}^\phi_{\vec{u}}=\mathbf{J}_{\vec{u}}\,\mathbf{\Pi}_{\nabla\phi}$ [18]. The new definition for the energy should be:[7]

$$E[\vec{u}]\triangleq\int_{\mathbb{R}^m} e_\phi[\vec{u}]\,\delta(\phi(x))\,dx \tag{10}$$

Comparing (9) with the classical equations for harmonic maps, we can infer the implicit form of the Christoffel symbols, $\mathbf{\Gamma}^l_{ij}(\vec{u})=\frac{\partial^2\psi}{\partial u^i\partial u^j}(\vec{u})\;\frac{\partial\psi}{\partial u^l}(\vec{u})$.[8]

4.3 Generic (Implicit) Domain Manifold and p-Harmonic Maps

Using both generalizations presented above, we arrive at the following formula with a bit more computational effort

$$\vec{u}_t = p^{1-\frac{2}{p}}\;\mathbf{\Pi}_{\nabla\psi(\vec{u})}\left(\nabla\cdot\left((e_{\phi,p}[\vec{u}])^{1-\frac{2}{p}}\;\mathbf{\Pi}_{\nabla\phi}\mathbf{J}^T_{\vec{u}}\right)\right) \tag{11}$$

where $e_{\phi,p}[\vec{u}]\triangleq\frac{1}{p}\|\mathbf{J}^\phi_{\vec{u}}\|^p_{\mathcal{F}}$.

A number of important examples of these general formulas are provided in [18]. In particular, we present how to process data constrained to be a direction (unit norm) and to be either normal or tangent to the domain manifold, e.g., [3]. This is an extremely important case, for example to denoise principal directions and normal vectors. To the unit constraint we of course add the fact that the data has to be tangent or normal to the manifold, an important constraint that was not included in [3].

5 Numerical Implementation and Examples

We now briefly discuss the numerical implementation of the flows previously introduced. Since the target manifold is now implicitly represented, we can basically use classical, well studied, numerical techniques on Cartesian grids. In other words, the framework here introduced permits the use of already existing numerical techniques, thereby enjoying their available analysis results. This is a key concept, instead of working on the development of new numerical schemes for meshes, the use of implicit representations following our framework brings us back to classical schemes. Moreover, examples like those in Figure 1 have not been reported in the literature yet, since prior to our approach all PDE's for mapping 3D meshes used projections as intermediate steps. Therefore, the work here proposed, when combined with [3],

[7]We have already taken into account that $\|\nabla\phi\|=1$.

[8]Of course $g^{ij}=\left(\mathbf{\Pi}_{\nabla\phi}\right)_{ij}\;(=g^{-1}_{ij})$. Then, it is nice to observe (although formally incorrect) that since $\mathbf{\Pi}_{\nabla\phi}\nabla\phi=0$, then the metric $g:\mathbb{R}^d\to\mathbb{R}^{d\times d}$ has eigenvalue $+\infty$ in the direction given by $\nabla\phi$ thus prohibiting intermingling of information between adjacent level sets of ϕ.

not only permits to use classical numerical schemes to solve PDE's and variational problems for surfaces, it is also an enabling technology for general maps.

Note that although the flows derived in this paper guarantee that the map remains on the target (sub-manifold), numerical errors can move it away from it, requiring a simple projection step. In particular, when dealing with submanifolds, although the evolution equations also guarantee that the solution will remain inside the convex hull, due to numerical discretization, $\vec{u}$ could be taken outside of it during the evolution. In order to numerically project it back, we need to have a distance function to this convex hull defined on the implicitly defined target manifold. In [17] we have shown how to computationally optimal compute such a distance function on implicitly defined manifolds, and this is the technique used for this projection into the convex hull.

An explicit scheme can be devised to implement (9). However, following [7], it turns out that it is more convenient to implement a *mathematically equivalent* formulation:

$$\frac{\partial u}{\partial t} = \Delta u \; - \; \big(\Delta u \cdot \nabla \psi\big) \nabla \psi \tag{12}$$

Proposition 5 ([18]) *Equation (12) is equivalent to the mapping into implicit surfaces flow corresponding to (3).*

Details on how this particular equation (and the flow for general domain and target manifolds) is numerically implemented, following classical Cartesian schemes, can be found in [18].

In all the examples below, the domain manifold $\mathcal{M}$ is either the Euclidean space $\mathbb{R}^2$ or an implicit torus. The target manifold $\mathcal{N}$ is an implicit surface in $\mathbb{R}^3$, that is, the zero level-set of $\psi : \mathbb{R}^3 \to \mathbb{R}$, ψ being a signed distance function (this is of course also the case when the surface is a sphere, ψ being as in §2.2).

In order to present interesting examples we construct texture maps, add noise to them, and then diffuse them using our framework. Let $\mathcal{S}$ be the surface onto which we want to map a given (planar) image defined in a subset $D \subset \mathbb{R}^2$. Then the *texture pap* is a map $\vec{T} : \mathcal{S} \to D$. Once the map is known, we inverted it to find a map $\vec{u}_0 : D \to \mathcal{S}$. Then, we built up the noisy map $\vec{u} : D \to \mathcal{S}$ defined by $\vec{u}(x) = \mathbf{\Pi}_{\mathcal{S}} \left(\vec{u}_0(x) + \vec{\mathbf{n}}(x)\right)$, where $\vec{\mathbf{n}} : D \to \mathcal{S}$ is random map with small prescribed power σ. We then feed the evolution equation with $\vec{u}$ as initial condition, and Neumann boundary conditions. After a certain number of steps, we stop the evolution, invert the resulting map, and use it as a texture map to paint the surface with a certain texture.[9]

As a means of finding a suitable $\vec{T}$ we have extended the work in [29] (a multidimensional scaling approach), combined with the technique developed in [17] for computing distances on implicit surfaces. In all the steps just described there are some minor implementation details, mainly regarding interpolation tasks, that we omit for the sake of clarity.

[9] Note that we are not proposing this as a complete texture mapping alternative, it is just to provide an illustrative example.

In Figure 2 we then denoise vectors from the plane $\mathbb{R}^2$ to a 3D surface defined as the zero level-set of $\psi : \mathbb{R}^3 \to \mathbb{R}$ and map a texture image to the surface using the obtained map. Note that the map is the one being processed, not the image itself.

We also show an example of diffusion of random maps from an implicit torus to the implicit bunny model, see Figure 1. As expected from the theory, when evolving this set with the harmonic flow, the set converges to a unique point. This particular example of mapping a given 3D surface to another one was previously addressed via artificial, distortion introducing, projections to the plane or sphere when the surfaces were represented as meshes [26].

6 Conclusions

In this paper we have shown how to implement variational problems and partial differential equations onto general target surfaces. We have also addressed the case of open target surfaces and sub-manifolds. The key concept is to represent the target (sub-)manifolds in implicit form, and then implement the equations in the corresponding embedding space. This framework completes the work with general domain manifolds reported in [3], thereby providing a complete solution to the computation of maps between generic manifolds.

References

[1] F. Alouges, "An energy decreasing algorithm for harmonic maps," in J.M. Coron *et al.*, Editors, *Nematics*, Nato ASI Series, Kluwer Academic Publishers, Netherlands, pp. 1-13, 1991.

[2] D. Adalsteinsson and J. A. Sethian, "Transport and diffusion of material quantities on propagating interfaces via level set methods," *Journal of Computational Physics* **185:1**, pp. 271-288, 2003.

[3] M. Bertalmio, L. T. Cheng, S. Osher, and G. Sapiro, "Variational problems and partial differential equations *Journal of Computational Physics*, **174:2**, pp. 759-780, 2001.

[4] V. Caselles, R. Kimmel, G. Sapiro, and C. Sbert, "Minimal surfaces based object segmentation," *IEEE-PAMI* **19:4**, pp. 394-398, April 1997.

[5] T. Chan and J. Shen, "Variational restoration of non-flat image features: Models and algorithms," *UCLA CAM-TR 99-20*, June 1999.

[6] R. Cohen, R. M. Hardt, D. Kinderlehrer, S. Y. Lin, and M. Luskin, "Minimum energy configurations for liquid crystals: Computational results," in J. L. Ericksen and D. Kinderlehrer, Editors, *Theory and Applications of Liquid Crystals*, pp. 99-121, IMA Volumes in Mathematics and its Applications, Springer-Verlag, New York, 1987.

[7] W.E and X.P. Wang, "Numerical methods for the Landau-Lifshitz equation," preprint.
`http://www.math.princeton.edu/~weinan`

[8] M. Eck and H. Hoppe, "Automatic reconstruction of B-spline surfaces of arbitrary topological type," *Computer Graphics (SIGGRAPH)*, 1996.

[9] J. Eells and L. Lemarie, "A report on harmonic maps," *Bull. London Math. Soc.* **10:1**, pp. 1-68, 1978.

[10] J. Eells and L. Lemarie, "Another report on harmonic maps," *Bull. London Math. Soc.* **20:5**, pp. 385-524, 1988.

[11] S. F. Frisken, R. N. Perry, A. Rockwood, and T. Jones, "Adaptively sampled fields: A general representation of shape for computer graphics," *Computer Graphics (SIGGRAPH)*, New Orleans, July 2000.

[12] B. Gustafsson, H.O. Kreiss, and J. Oliger, *Time Dependent Problems and Difference Methods*, John Wiley & sons inc.

[13] R. Hamilton, *Harmonic Maps of Manifolds with Boundary*, Lecture Notes in Mathematics **471**, Springer-Verlag, Berlin-New York, 1975.

[14] T. Kanai, H. Suzuki, and F. Kimura, "Three dimensional geometric metamorphosis based on harmonic maps," *The Visual Computer* **14:4**, pp.166-176, 1998.

[15] R. Kimmel and N. Sochen, "Orientation diffusion," *Journal of Visual Communication and Image Representation*, to appear.

[16] V. Krishnamurthy and M. Levoy, "Fitting smooth surfaces to dense polygon meshes," *Computer Graphics*, pp. 313-324, 1996.

[17] F. Mémoli and G. Sapiro, "Fast computation of weighted distance functions *Journal of Computational Physics*, **173:2**, pp. 730-764, November 2001.

[18] F. Mémoli, G. Sapiro, and S. Osher, "Solving variational problems and partial differential equations mapping into general target manifolds," *IMA Report* **1827**, January 2002 (http://www.ima.umn.edu/).

[19] F. Mémoli and G. Sapiro "Harmonic brain warping," in preparation.

[20] S. J. Osher and J. A. Sethian, "Fronts propagation with curvature dependent speed: Algorithms based on Hamilton-Jacobi formulations," *Journal of Computational Physics* **79**, pp. 12-49, 1988.

[21] A. Pardo and G. Sapiro, "Vector probability diffusion," *IEEE Signal Processing Letters* **8**, pp. 106-109, April 2001.

[22] P. Perona, "Orientation diffusion," *IEEE Trans. Image Processing* **7**, pp. 457-467, 1998.

[23] T. Sakai, *Riemannian Geometry*, AMS Translations of Mathematical Monographs, vol 149.

[24] B. Tang, G. Sapiro, and V. Caselles, "Diffusion of general data on non-flat manifolds via harmonic maps theory: The direction diffusion case," *Int. Journal Computer Vision* **36:2**, pp. 149-161, February 2000.

[25] J. W. Thomas, *Numerical Partial Differential Equations, Finite Difference Methods*, Texts in Applied Mathematics, 22. Springer Verlag, 1995.

[26] A. W. Toga, *Brain Warping*, Academic Press, New York, 1998.

[27] G. Yngve and G. Turk, "Creating smooth implicit surfaces from polygonal meshes," *Technical Report GIT-GVU-99-42, Graphics, Visualization, and Usability Center. Georgia Institute of Technology*, 1999.

[28] D. Zhang and M. Hebert, "Harmonic maps and their applications in surface matching," *Proc. CVPR '99*, Colorado, June 1999.

[29] G. Zigelman, R. Kimmel, and N. Kiryati, "Texture mapping using surface flattening via multi-dimensional scaling," *Technion-CIS Technical Report* **2000-01**, 2000.

[30] L. A. Vese and S. J. Osher, "Numerical methods for p-harmonic flows and applications to image processing," *CAM-UCLA Report* **01-22**, August 2001 (to appear in *SIAM. J. Numerical Analysis*).

[31] J. Weickert, *Anisotropic Diffusion in Image Processing*, ECMI Series, Teubner-Verlag, Stuttgart, Germany, 1998.

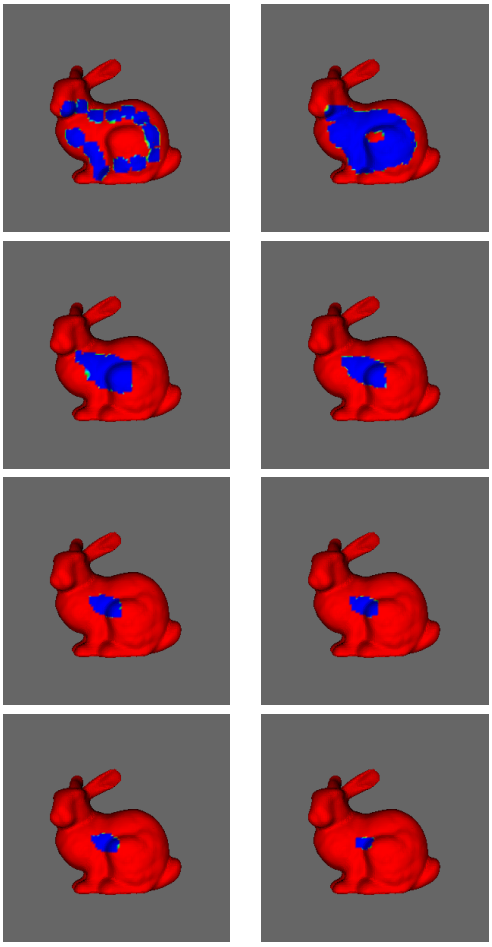

Figure 1: Diffusion of a random map from an implicit torus to the implicit bunny. In blue are marked those points of the bunny's surface pointed by the map at every instant. Different figures correspond to increasing instances of the evolution, from top to bottom and left to tight. We show the map at samples of 100 iterations performed to the initial map with a time step of .01. We used the 2-harmonic heat flow with adiabatic conditions. *(This is a color figure.)*

Figure 2: First row: Diffusion of a noisy texture map (left) onto an implicit sphere (right). Second row: Diffusion of a noisy texture map onto an implicit teapot. We show two different views. Third row: Diffusion of a texture map for an implicit teapot. *(This is a color figure.)*